A Novel Soft Glove Utilizing Honeycomb Pneumatic Actuators (HPAs) for Assisting Activities of Daily Living

Jianwei Lai, Aiguo Song, *Senior Member, IEEE*, Jiajin Wang, Ye Lu, Ting Wu, Huijun Li, Baoguo Xu, *Member, IEEE*, and XiangShan Wei

***Abstract*— Fabric-based pneumatic actuators (FPAs) are extensively employed in the design of lightweight and compliant soft wearable assistive gloves. However, conventional FPAs typically exhibit limited output force, thereby restricting the applications of such gloves. This paper presents the development of a novel honeycomb pneumatic actuator (HPA) constructed using flexible thermoplastic polyurethane (TPU) coating through hot pressing or ultrasonic welding techniques. Compared to the previously utilized double-layer fabric-based pneumatic actuators (DLFPAs), the HPAs yields a remarkable 862% increase in end output force. It can produce a tip force of 13.57 N at a pressure of 150 kPa. The integration of HPAs onto a soft pneumatic glove enables the facilitation of various activities of daily living. A series of trials involving nine patients were conducted to assess the effectiveness of the soft glove. The experimental results indicate that when assisted by the glove, the patients' finger metacarpophalangeal (MCP) and proximal interphalangeal (PIP) joints achieved angles of 87.67 ± 19.27° and 64.2 ± 30.66°, respectively. Additionally, the average fingertip force reached 10.16 ± 4.24 N, the average grip force reached 26.04 ± 15.08 N, and the completion rate of daily functions for the patients increased from 39% to 76%. These outcomes demonstrate that the soft glove effectively aids in finger movements and significantly enhances the patients' daily functioning.**

***Index Terms*— Pneumatic actuators, rehabilitation robotics, wearable robotics, soft robot materials and design.**

Manuscript received 13 June 2023; revised 27 July 2023; accepted 2 August 2023. Date of publication 7 August 2023; date of current version 11 August 2023. This work was supported in part by the National Natural Science Foundation of China under Grant 92148205 and Grant 62173088 and in part by the Frontier Leading Project of Jiangsu Basic Research Program under Grant BK20192004. *(Corresponding author: Aiguo Song.)*

This work involved human subjects or animals in its research. Approval of all ethical and experimental procedures and protocols was granted by the Medical Ethics Committee under Application No. 2020ZDSYLL088-P01.

Jianwei Lai, Aiguo Song, Jiajin Wang, Ye Lu, Huijun Li, and Baoguo Xu are with the State Key Laboratory of Bioelectronics, Jiangsu Key Laboratory of Remote Measurement and Control, School of Instrument Science and Engineering, Southeast University, Nanjing 210096, China (e-mail: a.g.song@seu.edu.cn).

Ting Wu is with the Department of Neurology, The First Affiliated Hospital of Nanjing Medical University, Nanjing 210029, China (e-mail: wuting80000@126.com).

XiangShan Wei is with the Department of Rehabilitation, Zhongda Hospital affiliated of Southeast University, Nanjing 210096, China (e-mail: 3242975593@qq.com).

Digital Object Identifier 10.1109/TNSRE.2023.3302612

I. Introduction

STROKE is a prevalent condition among the elderly population, leading to severe hand motor dysfunction that significantly impacts their ability to carry out activities of daily living (ADLs) and, consequently, their overall quality of life [1]. Presently, many patients heavily rely on the support of their family members or healthcare workers to accomplish daily tasks, placing a considerable burden on both the patient and their family [2]. However, with the rapid advancements in rehabilitation robotics, a promising solution for rehabilitation training and daily living assistance is emerging [3]. Numerous hand rehabilitation robots have been developed to aid patients in their rehabilitation process [4], [5]. Moreover, some of these rehabilitation robots can extend their assistance to support patients in performing daily life functions [6], [7].

In traditional hand-assisting robots, the primary approach has been through rigid exoskeletons that utilize linkage structures to provide precise finger position or force assistance for patients. For instance, Hong et al. developed the KULEX-Hand, which enables natural grasping assistance for the patient's fingers [8]. Similarly, Li et al. designed an underdriven hand exoskeleton employing an admittance control algorithm to enhance the exoskeleton's flexibility in assisting the patient's finger movements during grasping tasks [9]. However, both the KULEX-Hand and Li's underdriven exoskeleton are limited in their functionality, as they can only assist the movement of the thumb and index finger. Consequently, they may not adequately meet the diverse demands of patients' daily activities. To address these limitations, Xu et al. developed a five-degree-of-freedom hand exoskeleton robot, which relies on a data-driven control algorithm to achieve precise force control [10]. Nonetheless, despite these advancements, existing rigid exoskeletons encounter additional challenges such as substantial mass in the wearing part and an inability to adapt to fingers of varying sizes. These issues pose restrictions on the broader application of hand-assisting robots.

Soft pneumatic gloves have gained considerable attention as promising tools due to their low stiffness and excellent flexibility [11], [12], [13]. Chen et al. proposed a multi-cavity soft actuator structure that utilizes the substantial deformation of the inner soft actuator and mutual extrusion to achieve bidirectional bending [14]. The bending angle and output force of the soft actuator increase with elevated air pressure. Polygerinos et al. developed a soft wearable glove comprising actuators constructed from molded silicone elastomeric chambers reinforced with fibers [15]. This actuator enables complex movements resembling those of human fingers in multiple directions through a single air pressure input. However, generating sufficient contact force for hand rehabilitation remains challenging due to the limited pressure-bearing capacity of silica gel. There are a number of methods that have been employed to develop actuators with large output forces, including fabric reinforcement [16], fiber reinforcement [17], and increased thickness of the silica gel in the cavity [18]. Nevertheless, these methods lead to larger actuator size and mass. Additionally, they impose higher demands for air pumps to generate the necessary air pressure, thereby posing challenges to the portability of the robotic rehabilitation system.

Several research groups have successfully developed soft assistive gloves incorporating fabric-based pneumatic actuators (FPAs) that have high output forces [19], [20], [21]. Compared to actuators based on silicone materials, FPAs offer advantages such as smaller size and higher pressure-bearing capacity. Yap et al. introduced a soft glove utilizing FPAs [22]. The weight of the soft glove is 99 g, while the total weight of the control system is 1.72 kg. Feng et al. proposed an FPA design with asymmetric chambers and an interference-reinforced structure to enhance the actuator's output force [23]. However, the inclusion of rigid gaskets in the design increases the thickness and weight of the actuator, posing challenges in manufacturing. Currently, most FPAs developed for hand-assistive gloves adopt a double-layer structure comprising a flexion airbag and an extension airbag [19], [22], [23]. These double-layer structure fabric-based pneumatic actuators (DLFPAs) facilitate finger movement in both flexion and extension directions. Nevertheless, during the inflation process of the flexion and extension airbags, stress arises between the two airbags, limiting the output force and bending angle of the DLFPAs.

Based on the comprehensive review outlined above, the majority of current soft actuators rely on controlling the deformation of the soft material to achieve rotation in a specific direction. This deformation is induced by increasing air pressure within the actuator's inner cavity, enabling the desired rotation through mutual extrusion among the elastic materials. However, these actuators face several challenges. Firstly, a portion of the work performed by the soft actuator is stored as deformation within the actuator itself, leading to energy loss during reciprocating motion. Secondly, soft materials undergo significant strain and volume changes during braking, potentially resulting in fatigue and compromising the actuator's durability. Lastly, the flexing of soft actuators relies on the deformation of the cavity inside the actuator, rendering them dependent on large air pressures.

Fig. 1. Soft pneumatic glove rehabilitation system with HPAs for assisting activities of daily living.

To address these issues, this paper introduces a novel honeycomb pneumatic actuator (HPA) that incorporates a simulated honeycomb structure. The movement of the actuator is based on the flexion and folding of the airbag, reducing the reliance on cavity deformation and mitigating the need for high air pressure. Moreover, the honeycomb structure of the actuator includes a centrally located guide layer, effectively alleviating stress between the flexion and extension airbags. This design enhancement enables increased bending angles and output force. Consequently, the actuator exhibits reduced pressure requirements on the air pump, resulting in enhanced efficiency and wear resistance.

This paper focuses on the development of a novel soft pneumatic glove based on HPAs for assisting daily living activities. The design, manufacturing process, and effectiveness evaluation of the HPAs have been thoroughly investigated. The main contributions of this research can be summarized as follows:

1) Proposal of a HPA: The honeycomb structure of the actuator includes a guide layer located in the middle, which effectively relieves the stress between the flexion and extension airbag, resulting in improved output force and bending angle of the HPA.
2) Creation of a soft pneumatic glove based on HPAs: The developed glove serves as an assistive tool for stroke patients in daily life activities, as shown in Fig. 1. The efficacy of the glove in facilitating grasping ability and daily living skills has been validated.
3) Developed of two test devices for finger force information, including finger tip force and hand grip force. This provides an effective tool for quantifying finger function in patients.

II. Honeycomb Pneumatic Actuator

A. Actuator Design

The honeycomb structure consists of interconnected regular hexagons, which inherently possess deformability. However,

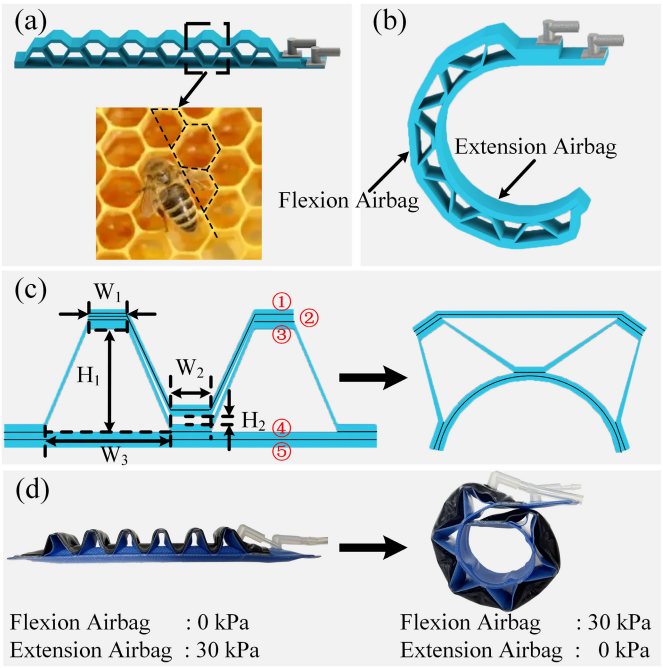

Fig. 2. Schematic diagram of the HPA. (a) Extension state. (b) Flexion state. (c) joint Parameters: Red numbers indicate the number of layers of TPU materials. (d) Inflation of the flexion and extension airbags to achieve the flexion and extension states, respectively.

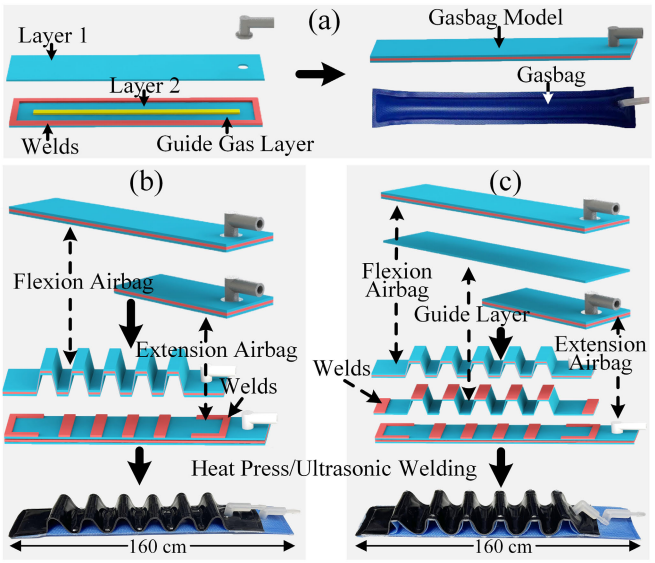

Fig. 3. Fabrication process of the soft actuator. Red represents welding parts, blue represents TPU material, and white represents gas pipe connectors. (a) Airbag fabrication process. (b) DLFPA fabrication process. (c) HPA fabrication process.

when arranged in a honeycomb configuration, the hexagons become tightly embedded and compactly interconnected, resulting in a stabilized shape for the overall structure. This unique arrangement imparts the honeycomb structure with advanced characteristics such as high strength and stiffness [24], making it suitable for various daily applications. Drawing inspiration from this, a honeycomb pneumatic actuator (HPA) is designed. The HPA utilizes flexible thermoplastic polyurethane (TPU), a smooth thermoplastic material that combines softness with minimal expansion. This unique material property helps minimize work loss caused by deformation within the actuator. Fig. 2(a) illustrates the extended state of the HPA, where the flexion airbag folds down, resulting in a compact actuator structure. To prevent any potential damage to the finger during extension, the lowest layer of the actuator is designed as a linear airbag, ensuring a maximum extension angle of 0°. The flexion state of the honeycomb structure soft actuator is depicted in Fig. 2(b), exhibiting a two-layer honeycomb structure.

The dimensional diagram of the soft actuator is presented in Fig.2(c). To optimize the actuator's performance, a preliminary experiment was conducted to determine the key parameters, yielding the following optimization results: The width of the joints between the flexion airbag and the guidance layer is denoted as $W_1 = W_2 = 5\ mm$. The height and width of the semi-hexagonal structure are represented as $H_1 = 13\ mm$ and $W_3 = 16\ mm$, respectively. The distance between the bottom of each ripple of the flexion airbags and the guide layer is defined as $H_2 = 1\ mm$. The overall width of the actuator is set to 25 mm, with the cavity width measuring 15 mm and the weld width measuring 5 mm. The proposed actuator comprises five layers of TPU materials. The first and second layers constitute a buckling airbag, while the third layer serves as a guidance layer. The fourth and fifth layers form the extension airbag. The soft actuator adopts a two-layer cellular structure, with the first layer consisting of regular hexagons as the fundamental units and the second layer composed of semi-hexagons. These units are arranged in a cellular pattern, collectively forming the overall structure of the actuator.

In the figure depicted in Fig.2(d), the flexion airbag and the extension airbag are individually inflated to achieve the flexion and extension states, respectively. Fig.2(c) provides a detailed illustration of the state transition. By virtue of the bending at each joint, the actuator with a consistent joint structure enables substantial bending movements. Importantly, it should be noted that the bending motion of the HPA relies on the extension or bending of the flexion airbag, rather than the expansion of the cavity. This movement approach effectively reduces the necessity for high air pressure within the cavity, thereby enhancing the actuator's output efficiency.

B. Actuator Fabrication

The fabrication process of the HPA is presented in Fig. 3. Each actuator comprises a flexion airbag and an extension airbag, with the airbag serving as the fundamental unit of the actuator. To prevent gas blockage between the two chambers, a small strip of TPU material measuring 2 mm wide and 180 mm long is incorporated in the middle of the airbag. The length of this small strip should cover every cavity of the actuator. An air nozzle is attached at the end of each airbag, allowing for connection to an air pipe to regulate the air pressure within the airbag. By separately inflating the flexion airbag and the extension airbag, the soft actuator can achieve the desired flexion and extension functionalities.

The fabrication process of an airbag is illustrated in Fig. 3(a). Firstly, the TPU material is laser cut into a CAD

TABLE I
COMPOSITION OF ACTUATORS

Actuator	Extension gasbag	Guide layer	Flexion gasbag
Do_TPU420D	TPU420D	-	TPU420D
Do_TPU70D	TPU420D	-	TPU70D
Ho_TPU420D	TPU420D	TPU140D	TPU420D
Ho_TPU70D	TPU420D	TPU140D	TPU70D

Do: Double-layer fabric-based pneumatic actuator, Ho: Honeycomb pneumatic actuator.

pattern, with the upper layer of TPU material marked with a thermal welding trace. Subsequently, a thermal welding machine is employed to weld the air nozzle onto the first layer of the airbag. The red strip in Fig. 3 represents the weld between the airbags. A guide gas layer is inserted between the first and second layers of TPU material to ensure smooth gas flow among the chambers formed by the bending of the airbag. Finally, the four edges of the airbag are sealed using a thermal welding machine, ensuring that the four layers of the airbag form a closed cavity.

The DLFPA, which is commonly used in soft pneumatic gloves [19], [22], [23], follows a specific fabrication process as depicted in Fig. 3(b). It consists of four TPU materials, including a flexion airbag and an extension airbag. The flexion airbag is corrugated, and then it is heat welded to the corresponding extension airbag positions, which include the bottom and both ends of the flexion airbag. In the DLFPA, the flexion airbag is in direct contact with the extension airbag.

In contrast, the fabrication process of HPA is different from that of DLFPA, as shown in Fig. 3(c). The HPA consists of five layers of TPU material, including a flexion airbag, a guide layer, and an extension airbag. First, the guide layer is corrugated, and then it is heat welded to the corresponding extension airbag positions, which include the bottom and both ends of the guide layer. Subsequently, the flexion airbag is heat welded to the corresponding position of the guide layer, and the weld positions include the top and both ends of the guide layer. The guide layer provides support for the movement of the flexion airbag and reduces the contact forces between the flexion and extension airbags. To achieve a compact and flexible actuator, the flexion airbag is bent downward.

In order to investigate the impact of different materials and structures on the output performance of soft actuators, we conducted an experiment involving the fabrication of four actuators. Table I provides an overview of the various actuator configurations. The term preceding the "_" symbol indicates the specific actuator structures, including DLFPA and HPA. The term following the "_" symbol corresponds to the materials utilized for the flexing airbag. For instance, the designation "Do_TPU420D" represents a DLFPA with a flexion airbag constructed from TPU420D material. As per previous research findings [19], Finger extension requires higher stiffness to provide sufficient output force. We selected a stiffer TPU420D for the extension actuator to ensure a sufficient extension force. The thermoplastic characteristics of TPU materials make heat welding a highly stable and reliable

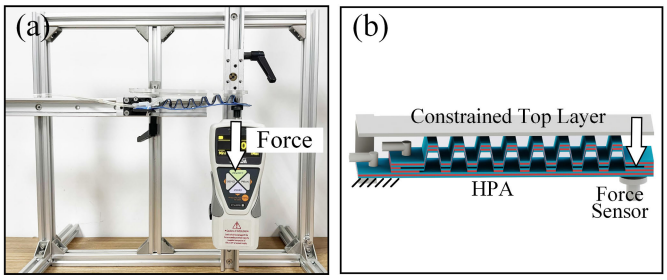

Fig. 4. Device for measuring soft actuators. (a) Device for measuring end output force in blocked state. (b) Schematic diagram of force measurement system for measuring the force of the blocking tip applied by HPA.

processing method. This technique ensures strong adhesion between the layers, resulting in robust actuators with enhanced durability. Moreover, the low processing cost of heat welding makes it a cost-effective manufacturing approach for large-scale production. To ensure comparability between actuators of different configurations, the key parameters in the HPA are kept consistent with those of the DLFPA, except for the absence of parameters W_2 and H_2.

C. Actuator Characteristic

This section evaluates the impact of different materials and structures on the end output force when the actuators are in a blocked state. The objective is to identify a sufficiently large drive that can overcome the patient's residual finger force and assist them with their daily living functions.

1) Method: The performance analysis involves conducting tests with varying air pressures applied within the actuators. The air pressure range is set from 0 to 150 kPa, with increments of 30 kPa, to observe the corresponding output performance of the actuators. To reduce experimental error, each assessment experiment was repeated three times.

To evaluate the tip-blocking force of the actuators, a measurement platform comprising a force sensor is set up. The platform consists of a movable two-axis motion platform and a force sensor (ZTS-50 N; Imada Co., Ltd., Toyohashi, Japan), as depicted in Fig. 4. One end of the actuator is brought into contact with the force sensor, while the other end is connected to the air pump for control. During pressurization, the actuator's surface comes into contact with the surface of the limiting platform, which helps constrain and minimize curvature changes in the actuator. This force measurement method is similar to the experimental approach employed in previous studies [18]. The use of a limiting surface for the actuator reduces nonlinear effects resulting from curvature changes during pressurization.

2) Result: The tip blocked force of the actuators is presented in Fig. 5(a). It can be observed that the tip blocked force of the soft actuators is directly proportional to the input air pressure, which aligns with the model established by O'Neill et al. [20]. In comparison to the double-layer actuators, the honeycomb actuators exhibit larger initial forces: Do_TPU420D and Do_TPU70D exhibit initial forces of 0.56 N and 0.06 N, respectively, while Ho_TPU420D and Ho_TPU70D exhibit initial forces of 1 N and 0.7 N, respectively. When

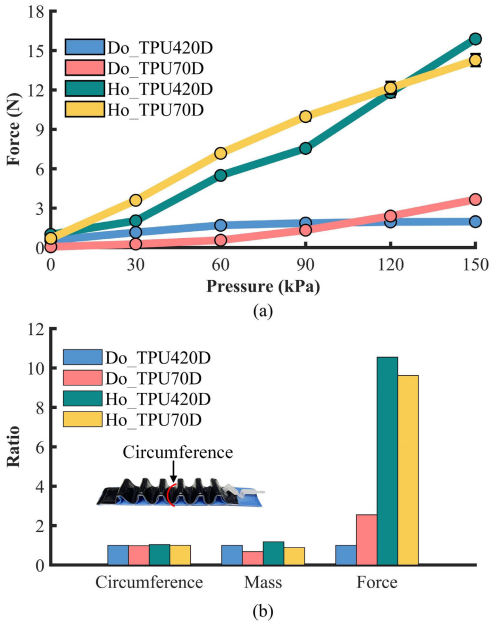

Fig. 5. Output force evaluation test results of multiple soft actuators. (a) End output force results for blocked condition of soft actuator. (b) Performance comparison results of multiple soft actuators vs. Do_TPU420D. The circumference refers to the measured length of the portion of the four actuators that exhibits the greatest difference in perimeter.

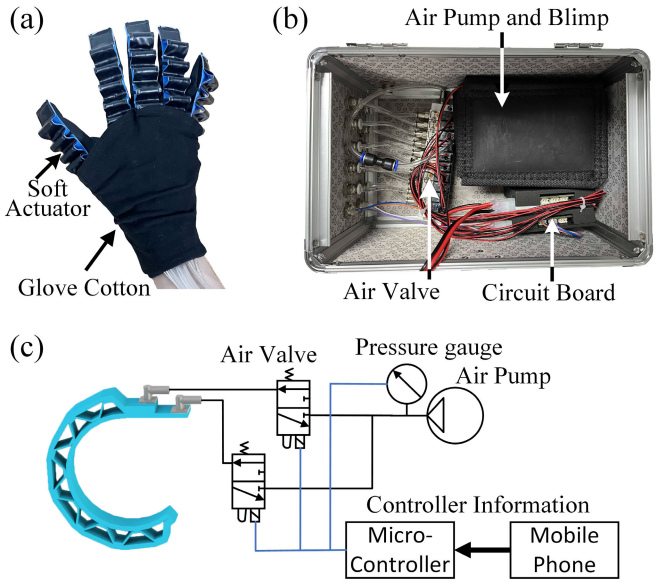

Fig. 6. Components of the soft pneumatic glove and control system. (a) Components of the soft pneumatic glove. (b) Control components of the soft actuator. (c) Control block diagram of the soft actuator.

excluding the initial force, the maximum tip blocked force of Ho_TPU420D reaches 14.88 N at an air pressure of 150 kPa. In comparison to Do_TPU420D, the maximum tip blocked force is increased by 155% (Do_TPU70D, 3.6 N), 906% (Ho_TPU420D, 14.88 N), and 862% (Ho_TPU70D, 13.57 N).

In conclusion, we conducted tests on the perimeter, mass, tip blocked force of the four actuators. When excluding the initial values, the force of the actuators are depicted in Fig. 5(b). The experimental results demonstrate that the mass and perimeter of the HPA are nearly identical to those of the DLFPA. It's worth noting that the HPA exhibits significantly improved output force without compromising the volume and mass of the DLFPA.

When considering the effect of the actuator's structure on its performance, the HPA demonstrates a significant increase in output force compared to the DLFPA. Turning to the impact of the actuator's material on performance, the actuator made of TPU70D for the DLFPA exhibits a significant improvement over the TPU420D variant, consistent with previous studies [19]. However, in the case of the HPA, the results for the TPU70D actuator are not significantly different from those of TPU420D. Considering the HPA's smaller initial force and mass, which enhances wearing comfort for patients, TPU70D is selected as the material for constructing the HPA with flexion airbags in the soft pneumatic gloves.

D. Actuator Integration

The soft pneumatic glove is composed of five soft actuators and a cotton glove, as illustrated in Fig. 6(a). To minimize resistance during finger movement, the actuators are attached to the cotton glove using elastic cords. The soft pneumatic gloves are designed with an open structure, as depicted in Fig. 7(a-b), allowing easy use for patients who have difficulty gripping. Additionally, the soft pneumatic glove feature Velcro stickers at both ends, enabling adjustment for patients with varying finger sizes. The soft pneumatic glove itself is made of fabric, while the actuators utilize soft materials, ensuring that the soft pneumatic glove avoids causing any secondary injury to the fingers. With a total weight of 107 g, the soft glove is remarkably lightweight compared to previous studies [12], [25], ensuring that it exerts minimal pressure on the patient's fingers. To accommodate individuals with different hand sizes, three types of cotton gloves have been integrated into the design: large, medium, and small. This approach empowers patients to select the glove that best suits their hand size, thereby ensuring an appropriate fit and facilitating ease of use during rehabilitation sessions.

The control system is housed in a modified medical box, as depicted in Fig. 6(b), designed for easy portability. The medical box is divided into two sections by a partition. The upper part of the box features a battery and four buttons, providing a storage space for the soft pneumatic glove when it is not in use. The lower part of the box contains an air pump, ten air valves, and a control circuit board. To minimize noise, the air pump is situated within sound insulation cotton. This measure can ensure that the operating noise of the system is less than 55 dB.

The pressure control system is represented in the schematic diagram shown in Fig. 6(c). The open-loop control method employed in this approach does not necessitate the installation of sensors on the glove, leading to a simplified and lightweight structure. This simplicity not only reduces the overall cost of the rehabilitation system but also enhances its robustness and reliability. The absence of sensors also eliminates the need for calibration and reduces potential maintenance requirements, making it a more user-friendly and practical solution for hand

TABLE II
DEMOGRAPHIC INFORMATION OF PATIENTS

Subject	Gender	Age	Time Post-stroke	ARAT(66)	MAS(4)
S1	M	81	8 days	9	1.5
S2	M	61	15 days	0	0
S3	M	65	37 days	0	0
S4	M	73	16 days	19	0
S5	M	56	19 days	0	0
S6	M	49	153 days	21	0
S7	M	73	28 days	3	1
S8	M	76	22 days	24	0
S9	F	52	132 days	19	0

ARAT: Action Research Arm Test, MAS: Modified Ashworth Scale.

rehabilitation. The control commands are initiated from a mobile phone and transmitted via Bluetooth to the microcontroller (STM32, ST Microelectronics, Geneva, Switzerland). The microcontroller regulates the air supply from the air pump (G4BL12170, Pengpu Co., Shanghai, China). This regulation is achieved through pulse width modulation (PWM), enabling precise control of the required air pressure. The air valve (LDC6V, OST Co., Ningbo, China) manages the pressure at the actuator's inlet. The entire system weighs approximately 1.8 kg.

III. EXPERIMENT

Experiments were conducted at the Affiliated Zhongda Hospital of Southeast University to assess the efficacy of the soft pneumatic glove in providing hand assistance. The research plan received approval from the Medical Ethics Committee (Ethics Approval No: 2020ZDSYLL088-P01). Prior to participating in the study, all patients provided written informed consent, indicating their voluntary participation and understanding of the research procedures.

A. Participants

The trial included a total of 9 stroke patients, comprising 8 men and 1 women, with an average height of 165 ± 18 cm and weight of 73 ± 15 kg. The inclusion criteria for the trial were as follows: (i) stroke diagnosis between 2 weeks and 3 years prior to the trial; (ii) age between 25 and 75 years; (iii) ability to understand movement instructions provided by the therapist; (iv) poor hand motor function of the affected joint, indicated by an Action Research Arm Test (ARAT) score of less than 35; (v) ability to undergo ARAT testing with the assistance of others. Patients were excluded if they had the following conditions: (i) mental disorder or expressive apraxia; (ii) severe cognitive impairment, indicated by a Mini Mental State Examination score of less than 23; (iii) severe spasticity of the affected joint, indicated by a Modified Ashworth Scale score of greater than 3; (iv) inability to move the fingers on the contralateral side, making it inconvenient to use the mobile phone for glove control. Table II provides the information of the recruited patients.

Fig. 7. Measurement diagrams and devices for finger movements and grip forces. (a) Index finger bending angle measurement diagram. (b) Thumb bending angle measurement diagram. (c) Fingertip force measurement device. (d) Finger grip force measurement device.

B. Glove-Assisted Range of Motion

The trial aims to assess the effect of soft gloves on the movement of patient fingers. To capture the joint positions, a 3D optical motion capture system (Optitrack, NaturalPoint Inc., Corvallis, Oregon, USA) was employed, with reflective markers placed on specific finger joints. The index finger's metacarpophalangeal (MCP), proximal interphalangeal (PIP), and distal interphalangeal (DIP) joints are marked, along with the interphalangeal (IP), MCP, and carpometa-carpal (CMC) joints of the thumb, as shown in Fig. 7(a-b).

During the trial, patients are instructed to wear soft glove on affected hands. The motion ranges of the fingers are recorded with and without the assistance of the glove. The process begins by establishing a baseline, recording the motion range of the patient's affected fingers. Next, the patient's fingers are observed without the aid of the soft glove. The extension airbag is then activated to assist the affected finger in returning to its extended state, followed by activating the flexion airbag to aid the finger in returning to its flexed state. To measure the motion range, the patients perform one cycle of finger movement. This cycle consists of moving the finger from its extended position to the flexed position and back to the extended position. The motion range is measured during this cycle. Each patient repeats this finger movement cycle five times to record the maximum motion range achieved.

By comparing the assisted finger movement with the non-assisted finger movement, the trial provides valuable insights into the efficacy of the soft glove in improving finger motion.

C. Glove-Assisted Grasp Strength

1) Fingertip Force: To assess the impact of the soft glove on the fingertip force of the patient's finger, a fingertip force

measurement device was specifically developed (Fig. 7(c)). The device comprises five force sensors (DYLY-109, DAYANG Inc., China) and a support frame. The accuracy of the force sensors is 0.1N and the measurement range is 0-50N.

The support frame consists of two main parts: the force measuring part and the palm contact part. The force measuring part is a square octagonal support structure featuring a slot in the middle, which facilitates the proper positioning of the sensors. On the other hand, the palm contact part is a hemisphere with a silicone coating on its spherical surface, achieved through an inverse molding technique. This design enables the device to adapt to the size of the patient's palm.

The position of the force sensors on the support frame can be adjusted to accommodate glove of different sizes worn by patients. Furthermore, the force measurement support frame can be modified for use on both the left and right hands by simply substituting the sensor accordingly.

During the experiment, volunteers hold the fingertip force measurement device in their hands and position each fingertip on the corresponding force sensor. They then perform a gripping action for a duration of 30 seconds. The force information captured by the sensors is recorded through a computer program dedicated to the task.

2) Grip Force: To assess the impact of the soft glove on the patient's finger grip, a force measurement device was devised. The device comprises a barometer (HT1895, XINGSITE Inc., Yantai, China) and an elastic pressure ball, as depicted in Fig. 7(d). The elastic pressure ball is a modified version of the pressure ball utilized in the sphygmomanometer, chosen for its affordability and user-friendliness.

By removing the check valve present in the elastic pressure ball, the air pressure inside the ball can be directly measured. To ensure continuous application of force by the patient to the elastic pressure ball, the air outlet at the bottom of the ball is blocked. Prior to the actual experiments, pre-tests were conducted to calibrate the force measurement device. Through these calibration tests, a relationship between the grip force F and the air pressure P was established: $F = kP + b$. In this equation, the elasticity coefficient of the dynamometer is denoted as k = 1.99, and the minimum force coefficient (b = 2.45) represents the minimum force required to induce a change in air pressure inside the pressure ball. One limitation of this force measurement device is its ability to detect a minimum force of only 2.4 N. However, the soft glove offers a significantly higher grip force than this value, rendering this limitation negligible for the purposes of the evaluation.

During the experiment, the patient grasps the elastic pressure ball and performs a fist-clenching action for a duration of 30 seconds. The peak air pressure achieved is observed on the display located above the barometer, and the corresponding finger grip force is then calculated.

D. Performance of ADLs With Glove Powered

The trial was designed to evaluate the impact of soft pneumatic glove on the hand function of patients in their daily lives. The trial design was based on the Action Research Arm Test (ARAT) scale and previous research findings [12].

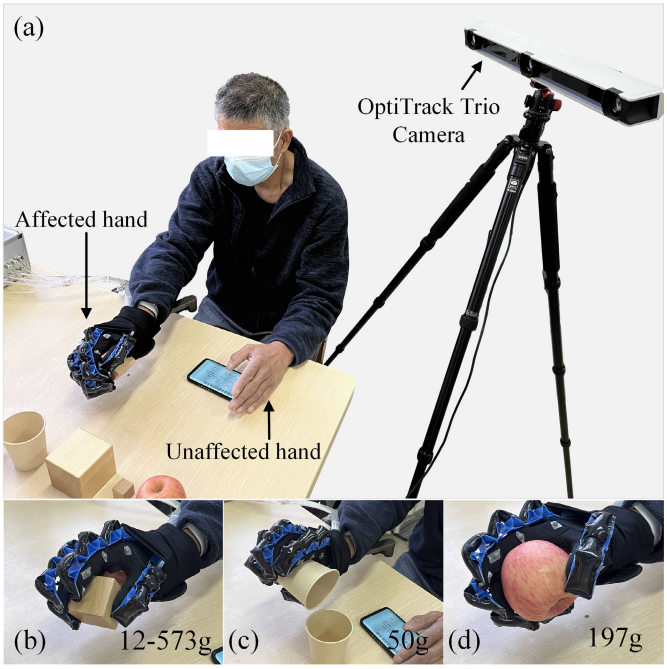

Fig. 8. Evaluation of the soft glove. (a) Schematic diagram of system evaluation. (b) Grip of block of wood with soft glove-assisted finger. (c) Pouring water with soft glove-assisted finger. (d) Grasping an apple with soft glove-assisted finger.

It consisted of three specific tasks aimed at assessing finger grasping ability and daily living skills.

The finger grasping task comprised four subtasks, involving the grasping of four square wooden blocks with side lengths of 2.5 cm, 5 cm, 7.5 cm, and 10 cm, respectively. To be considered successful, volunteers needed to pick up the wooden block and place it at a designated endpoint located 20 cm from the starting point without dropping it.

The daily life tasks included the apple catching task and the water pouring task. In the apple catching task, an apple weighing 197 g was used. Volunteers were required to grab the apple and place it at the designated endpoint 20 cm away without dropping it. If the apple was dropped or not placed correctly, it was considered a failure.

For the water pouring task, volunteers were instructed to pour the water from one cup to another. The combined mass of the cup and water was 50 g. Success in this task was determined by the absence of any spillage during the pouring process. If water was spilled, it was considered a failure.

Each sub-task had a time limit of 120 seconds, and if the time limit was exceeded, the sub-task was deemed unsuccessful. Each sub-task was performed five times, and if the task was successfully completed three or more times, it was recorded as a score of 1; otherwise, it was recorded as a score of 0.

E. Experimental Paradigm and Tasks

The experiment consisted of three phases: the preparation phase, the baseline testing phase, and the experimental phase.

In the preparation phase, several tests were conducted on the patients without wearing soft glove. These tests included measuring finger flexion angle, finger output force, and performing

the three tasks. After the initial testing, the patients then wore the soft glove on the affected finger. Using the healthy side finger to operate a phone, the patient's affected finger was controlled through commands to complete the tasks with the assistance of the soft glove. This phase aimed to familiarize the patient with the tasks and allow for practice with and without the glove assistance. The duration of this phase was 20 minutes.

During the baseline testing phase, the patients performed tests for finger flexion angle, finger output force, and the three tasks without wearing the soft gloves. This phase provided a baseline measurement of the patients' performance without the glove.

In the experimental phase, the patients wore the soft glove on the affected fingers. They operated the phone using the healthy side finger, while the affected finger was controlled through commands to complete the tests for finger flexion angle, finger output force, and the three tasks with the assistance of the soft glove.

It's important to note that for some volunteers with poor upper limb function (shoulder, elbow, and wrist), the assistance of a therapist was required for upper limb movement during the tasks. The preparation phase was completed once, and to minimize measurement errors, the entire trial was performed five times. A 3-minute break was taken between each task, and a 10-minute break was taken between the two phases to prevent muscle damage and eliminate errors caused by muscle fatigue.

F. Data Analysis

The collected data from the experiment were analyzed using Matlab. Patients were divided into two groups based on their ARAT scores: the low-functioning group (G1) consisting of patients 1, 2, 3, 5, and 7, and the high-functioning group (G2) consisting of patients 4, 6, 8, and 9. The mean and variance of the measured parameters were calculated for each group to assess their performance with and without the soft glove. To determine if there were significant differences between the groups, one-way ANOVA was applied. This statistical analysis helps quantify the effect of the soft glove on patients with different levels of assistance and provides insights into its effectiveness in improving hand function.

IV. Results

A. Range of Motion

The results depicted in Fig. 9 demonstrate the effect of the soft glove on finger movement space. Without the assistance of the glove, the finger motion space was found to be smaller. Specifically, for the index finger, the average range of motion was 46.67 ± 40.9°, 30.44 ± 26.49°, and 16.56 ± 13.26° for the MCP, PIP, and DIP joints, respectively. Regarding the thumb, the average range of motion for the MCP, IP, and CMC joints was 18.78 ± 12.11°, 15.33 ± 10.63°, and 11.78 ± 11.39°, respectively. However, with the assistance of the H0_TPU70D soft glove, significant improvements in finger motion space were observed. For the index finger, the average range of motion increased to 87.67 ± 19.27° (p = 0.015),

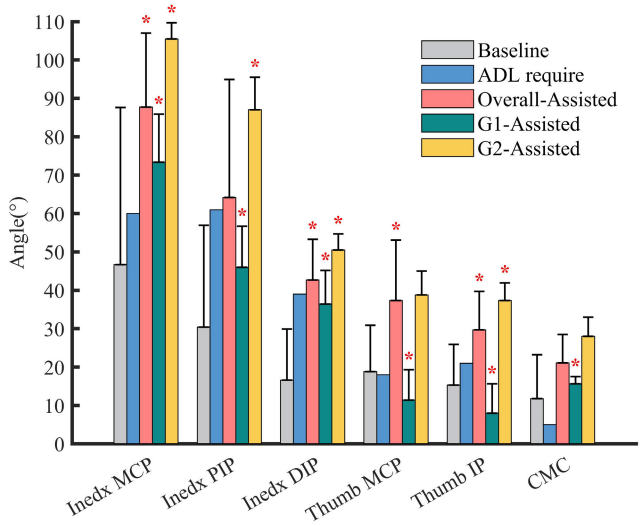

Fig. 9. Results of finger flexion angle test with and without soft glove for patient's finger. Significant differences ($p < 0.05$) are marked with *.

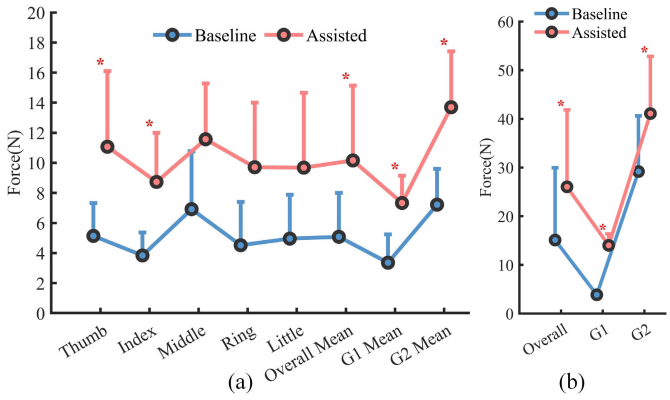

Fig. 10. Results of fingertip force and grip strength tests with and without soft gloves for patients' fingers. (a) Fingertip force: overall patients and mean fingertip force of G1 and G2 patients. (b) Finger grip strength: mean grip strength for overall, G1, and G2 patients. Significant differences ($p < 0.05$) are marked with *.

64.2 ± 30.66° (p > 0.05), and 42.7 ± 10.63° (p = 0.001) for the MCP, PIP, and DIP joints, respectively. As for the thumb, the mean range of motion was 37.33 ± 15.8° (p = 0.013), 29.67 ± 9.99° (p = 0.009), and 21.11 ± 7.36° (p = 0.055)for the MCP, IP, and CMC joints, respectively. These values are significantly larger than those reported in previous studies [22], indicating the effectiveness of our soft glove in assisting patients' finger movements. It is worth noting that the range of motion provided by the glove-assisted fingers exceeded the average functional range of motion of the hand, which is approximately 39° for finger DIP, 60° for PIP, 61° for MCP, 18° for thumb IP, and 21° for thumb MCP. These results indicate that the range of motion facilitated by the soft glove is sufficient for patients to perform more than 90% of their daily functional activities [26], [27].

B. Grasp Strength

1) Fingertip Force: The results of the effect of the soft glove on the patient's fingertip force are presented in Fig. 10(a).

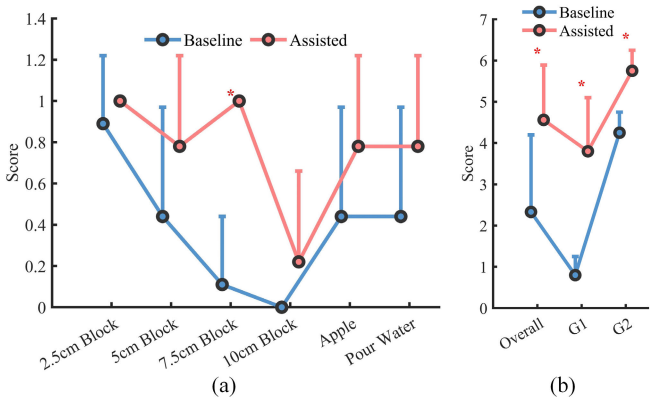

Fig. 11. Results of daily living function test with and without soft glove for patient's fingers. (a) Mean completion results for each subtask. (b) Task completion for overall, G1, and G2 patients. Significant differences ($p < 0.05$) are marked with *.

Without the soft glove, the patients exhibited fingertip output forces for the thumb, index finger, middle finger, ring finger, and little finger with an average of 5.14 ± 2.19 N, 3.84 ± 1.54 N, 6.92 ± 3.85 N, 4.53 ± 2.89 N, and 4.96 ± 2.92 N, respectively. However, when the patients used the soft glove, which significantly improved their finger range of motion, there was a noticeable increase in fingertip output forces. With the assistance of the soft glove, the patients achieved fingertip output forces of 11.08 ± 5.03 N ($p = 0.047$), 8.74 ± 3.28 N ($p = 0.028$), 11.58 ± 3.72 N ($p = 0.243$), 9.72 ± 4.29 N ($p = 0.172$), and 9.69 ± 4.98 N ($p = 0.173$) for the thumb, index finger, middle finger, ring finger, and little finger, respectively.

2) Force of Grasp: The results of the effect of the soft glove on the patient's finger grip force are depicted in Fig. 10(b). Without the soft glove, the patient's finger grip force measured an average of 15.11 ± 14.84 N. It is worth noting that this value is lower compared to the fingertip force due to the smaller diameter of the soft pressure ball used in the measurement. The patients experienced difficulty in gripping objects with their impaired fingers. However, when the patients used the soft glove, there was a significant improvement in finger grip strength. The finger grip force with the assistance of the soft glove increased noticeably. On average, the patient's hand grip strength improved by 10.93 ± 3.21 N. These values surpass those reported in similar studies [12], highlighting the superior performance of the actuator in our proposed program.

C. Performance of ADLs

The impact of the soft glove on patients' daily functioning was assessed through six subtasks, and the average patient scores for each task and overall scores are presented in Fig. 11. In the baseline condition without the soft glove, patients demonstrated relatively good performance in completing the 2.5 cm block task, with an 89% completion rate. However, the tasks involving the 5 cm block, grasping apples, and pouring water were poorly completed, with only approximately 40% of patients able to accomplish them. The challenges increased further with the 7.5 cm block and 10 cm block tasks, as they were barely completed by the patients. With the assistance of the soft glove, a significant improvement in task completion was observed. Most patients were able to successfully complete the tasks of grasping the 2.5 cm block, 5 cm block, 7.5 cm block, grasping apples, and pouring water. Although the 10 cm block remained challenging, a small number of patients were able to complete it. This task represents an extreme challenge in the ARAT assessment.

V. Discussion

A. Analysis of Experimental Results

The results pertaining to the motion range indisputably demonstrate that the baseline finger range of motion exhibited by the patients was inadequate for daily living activities. With the assistance of the soft glove, there was a significant improvement in the motion space of all five fingers, with an average increase of 21.26 ± 18.41°. Notably, both the G1 and G2 patients experienced significant improvements compared to their baseline levels. Specifically, the G1 patients demonstrated a remarkable increase of 26.7 ± 20.63° in their finger motion space with the soft glove. On the other hand, the G2 patients also exhibited an improvement of 14.67 ± 12.96°. These changes were statistically significant for both groups compared to their respective baseline levels. Moreover, the use of the soft glove resulted in a larger motion space for the fingers, accompanied by a smaller standard deviation, indicating a more consistent and reliable improvement compared to the baseline measurements. This observation is particularly pronounced in the G1 patients, suggesting that the soft glove had a greater impact on low-functioning group.

Upon comparing the grasp force results before and after using the soft glove, a notable improvement in patients' fingertip forces is evident, with an average increase of 5.08 ± 2.55 N observed when assisted by the glove. Specifically, the G1 patients experienced an increase of 3.97 ± 1.28 N, while the G2 patients demonstrated a more significant improvement of 6.47 ± 3.05 N. The reason behind the greater improvement in fingertip force with the soft glove is attributed to the high-functioning group patients' ability to control the direction of finger force. This control ensures that the force exerted by the soft actuator is applied vertically on top of the force sensor, enhancing the actuator's efficiency. Overall, the soft glove proved to be effective in increasing fingertip force for the patients, with the improvement being more prominent in the high-functioning group. This enhancement in fingertip force has the potential to enhance the patients' ability to perform daily tasks that require grip strength and precision.

The higher grasping force achieved with our HPA emphasizes its potential for providing enhanced support and assistance to patients during gripping tasks. Specifically, the G1 patients demonstrated an improvement of 10.15 ± 2.21 N, while the G2 patients exhibited a slightly higher improvement of 11.91 ± 4.03 N. This suggests that the effect of the soft glove on the patient's finger grip strength was consistent across both groups. These results indicate that the soft glove effectively enhanced the patient's finger grip strength, enabling them to exert more force while gripping objects. This improvement in finger grip strength has the potential to enhance the

TABLE III
COMPARISON OF REHABILITATION ROBOTS

Typical exoskeleton	Number of finger	Mechanism	Wearable weight (g)	Fingertip force (N)	Pressure(kPa)	Driving direction
Hong *et al.* [8]	1	Linkage	172	10	-	Flexion & Extension
Tran *et al.* [28]	2	Tendon	131	6.3	-	Flexion
Butzer *et al.* [29]	5	Tendon	148	6.4	-	Flexion
Polygerinos *et al.* [15]	5	Penumatic	255	8	345	Flexion
Correia *et al.* [12]	5	Penumatic	122 - 149	5.5	172	Flexion & Extension
Feng *et al.* [23]	5	Penumatic	65.5 - 86.7	13.46	150	Flexion & Extension
Yap *et al.* [18]	5	Penumatic	-	11.18	200	Flexion
Chen *et al.* [25]	5	Tendon	200	10	-	Flexion & Extension
Lai *et al.* [30]	5	Penumatic	317.7	16.02	200	Flexion & Extension
Proposed	5	Penumatic	107	13.57	150	Flexion & Extension

patient's ability to perform activities that require a strong grip, such as holding objects or manipulating tools.

In the performance of ADLs, the Overall of the patient completion rate increased from 39% to 76% with the use of the soft glove. The G1 patients experienced a substantial improvement, with completion rates increasing from 13% to 63%. Similarly, the G2 patients exhibited a significant increase in completion rates, from 71% to 96%. These results highlight the effectiveness of soft gloves in assisting patients in improving their daily functioning. The glove's assistance allowed patients to perform tasks that were previously challenging or impossible, leading to a substantial increase in task completion rates.

Regarding the durability of the gloves, a parallel study was conducted, involving over 10 patients who utilized our soft gloves for rehabilitation purposes at home for a duration exceeding 1 month. Throughout this period, these patients diligently engaged in daily rehabilitation exercises, with the soft gloves providing necessary assistance. The study's results unequivocally showcase the stability and reliability of our proposed soft glove system.

B. Comparison With Typical Rehabilitation Robots

In the section above, the HPA is tested in comparison with existing FPAs. To effectively demonstrate the contribution of the proposed actuator, the advantages of the soft glove made of the HPA are compared with typical hand exoskeletons described in the literature, including linkage-based [8], cable-based [28], [29], and pneumatic systems [12], [15]. Table III provides a summary of these comparisons.

Linkage-based exoskeletons can assist finger movements and provide a larger output force. Furthermore, they enable finger movement in both flexion and extension directions. However, the linkage structure necessitates auxiliary drive and actuation structures, and the actuators are primarily located in the palm of the hand. The robots proposed by Hong et al. have masses of only 172 g [8], meeting the weight requirement for wearable rehabilitation devices (less than 500 g). Nonetheless, these robots can only assist one and three finger movements, respectively. When the number of assisted fingers increases to five, the challenges of structural design and portability arise.

On the other hand, cable-based hand rehabilitation robots position the actuator structure externally at other sites, reducing stress on the fingers. The hand rehabilitation robots proposed by Tran et al. and Butzer et al. weigh only 131 g and 148 g [28], [29], respectively, significantly reducing finger stress. However, these robots generate less fingertip force due to the low transmission efficiency of the tendons. Moreover, the cables used in cable-based systems face limitations in assisting finger movement in both directions, as they cannot generate bidirectional forces.

In contrast, hand rehabilitation robots based on pneumatic technology offer several advantages, notably their lightweight design and ease of wear. The simplicity and compactness of the pneumatic actuator allow for effective rehabilitation of all five fingers, making it a promising choice. The proposed actuator exhibits a fingertip end force of 13.57 N at 150 kPa pneumatic pressure, surpassing the performance of other studies, highlighting its high efficiency. Moreover, the proposed flexible glove, weighing only 107 g for the wearing part and 12 g for each individual actuator, showcases the honeycomb-like structure's benefits: simplicity and lightweight nature. Additionally, the proposed actuator successfully overcomes the limitation associated with conventional pneumatic actuators, enabling bidirectional movement of fingers. This feature is particularly crucial in the rehabilitation process of stroke patients. By conducting these comparisons, we gain valuable insights into the strengths and weaknesses of different hand exoskeleton types, including the proposed actuator.

C. Limitations and Future Works

Our future work will concentrate on further investigating the modeling of the HPA to enhance their accuracy and provide more refined assistance to patients. In addition, the study employed an open-loop control algorithm, which proves to be a practical and cost-effective solution for hand rehabilitation gloves, offering high stability and ease of use for patients. Nevertheless, it should be acknowledged that in specific contexts demanding intricate and accurate movements, the control accuracy of an open-loop system might fall short. In order to tackle this constraint, our future research will center on investigating flexible sensor-based closed-loop control algorithms [31]. The integration of closed-loop control holds the potential to enhance the precision and accuracy of the system, thereby facilitating finer and more controlled movements in everyday activities.

VI. Conclusion

In this paper, we have presented a novel soft hand rehabilitation robot designed to assist patients in their daily lives by facilitating finger flexion and extension movements. The primary contribution of this study lies in the development of a HPA. Unlike previous studies, our proposed actuator design incorporates a guide layer positioned between the flexion and extension actuators. Experimental results have demonstrated that the HPA exhibits only a marginal increase in volume and mass compared to the DLFPA, while delivering a remarkable 862% increase in end output force. These findings indicate that the inclusion of the guide layer effectively reduces tension between the flexing and extending airbags, thereby enhancing the overall performance of the actuator. Furthermore, we have fabricated a soft pneumatic glove based on the HPA and conducted a clinical trial involving 9 patients to evaluate the impact of the glove on their ability to perform daily finger movements. The results have revealed significant improvements in the bending angle, output force, and the patients' ability to perform various daily tasks, all achieved with the assistance of the soft glove. The HPA enhances the output performance of the pneumatic actuator without altering its volume and mass, enabling effective augmentation of the patient's finger capacity at a low pressure of 150 kPa.

References

[1] C. W. Tsao et al., "Heart disease and stroke statistics—2023 update: A report from the American heart association," *Circulation*, vol. 147, no. 8, pp. 93–621, 2023.

[2] P. Boyne et al., "Optimal intensity and duration of walking rehabilitation in patients with chronic stroke," *JAMA Neurol.*, vol. 80, no. 4, p. 342, Apr. 2023.

[3] K. Shi, A. Song, Y. Li, H. Li, D. Chen, and L. Zhu, "A cable-driven three-DOF wrist rehabilitation exoskeleton with improved performance," *Frontiers Neurorobotics*, vol. 15, Apr. 2021, Art. no. 664062.

[4] A. Demofonti, G. Carpino, L. Zollo, and M. J. Johnson, "Affordable robotics for upper limb stroke rehabilitation in developing countries: A systematic review," *IEEE Trans. Med. Robot. Bionics*, vol. 3, no. 1, pp. 11–20, Feb. 2021.

[5] X. Hu, A. Song, Z. Wei, and H. Zeng, "StereoPilot: A wearable target location system for blind and visually impaired using spatial audio rendering," *IEEE Trans. Neural Syst. Rehabil. Eng.*, vol. 30, pp. 1621–1630, 2022.

[6] B. Noronha and D. Accoto, "Exoskeletal devices for hand assistance and rehabilitation: A comprehensive analysis of state-of-the-art technologies," *IEEE Trans. Med. Robot. Bionics*, vol. 3, no. 2, pp. 525–538, May 2021.

[7] X. Chen et al., "A wearable hand rehabilitation system with soft gloves," *IEEE Trans. Ind. Informat.*, vol. 17, no. 2, pp. 943–952, Feb. 2021.

[8] M. B. Hong, S. J. Kim, Y. S. Ihn, G.-C. Jeong, and K. Kim, "KULEX-hand: An underactuated wearable hand for grasping power assistance," *IEEE Trans. Robot.*, vol. 35, no. 2, pp. 420–432, Apr. 2019.

[9] H. Li, L. Cheng, N. Sun, and R. Cao, "Design and control of an underactuated finger exoskeleton for assisting activities of daily living," *IEEE/ASME Trans. Mechatronics*, vol. 27, no. 5, pp. 2699–2709, Oct. 2022.

[10] W. Xu, Y. Guo, C. Bravo, and P. Ben-Tzvi, "Design, control, and experimental evaluation of a novel robotic glove system for patients with brachial plexus injuries," *IEEE Trans. Robot.*, vol. 39, no. 2, pp. 1637–1652, Apr. 2023.

[11] Z. Q. Tang, H. L. Heung, K. Y. Tong, and Z. Li, "Model-based online learning and adaptive control for a 'human-wearable soft robot' integrated system," *Int. J. Robot. Res.*, vol. 40, no. 1, pp. 256–276, 2021.

[12] C. Correia et al., "Improving grasp function after spinal cord injury with a soft robotic glove," *IEEE Trans. Neural Syst. Rehabil. Eng.*, vol. 28, no. 6, pp. 1407–1415, Jun. 2020.

[13] S. Terryn, J. Brancart, D. Lefeber, G. Van Assche, and B. Vanderborght, "Self-healing soft pneumatic robots," *Sci. Robot.*, vol. 2, no. 9, Aug. 2017, Art. no. eaan4268.

[14] W. Chen, C. Xiong, C. Liu, P. Li, and Y. Chen, "Fabrication and dynamic modeling of bidirectional bending soft actuator integrated with optical waveguide curvature sensor," *Soft Robot.*, vol. 6, no. 4, pp. 495–506, Aug. 2019.

[15] P. Polygerinos, Z. Wang, K. C. Galloway, R. J. Wood, and C. J. Walsh, "Soft robotic glove for combined assistance and at-home rehabilitation," *Robot. Auto. Syst.*, vol. 73, pp. 135–143, Nov. 2015.

[16] Y. Chen, X. Tan, D. Yan, Z. Zhang, and Y. Gong, "A composite fabric-based soft rehabilitation glove with soft joint for dementia in Parkinson's disease," *IEEE J. Transl. Eng. Health Med.*, vol. 8, pp. 1–10, 2020.

[17] H. Li, J. Yao, P. Zhou, X. Chen, Y. Xu, and Y. Zhao, "High-force soft pneumatic actuators based on novel casting method for robotic applications," *Sens. Actuators A, Phys.*, vol. 306, May 2020, Art. no. 111957.

[18] H. K. Yap, H. Y. Ng, and C.-H. Yeow, "High-force soft printable pneumatics for soft robotic applications," *Soft Robot.*, vol. 3, no. 3, pp. 144–158, Sep. 2016.

[19] L. Ge et al., "Design, modeling, and evaluation of fabric-based pneumatic actuators for soft wearable assistive gloves," *Soft Robot.*, vol. 7, no. 5, pp. 583–596, Oct. 2020.

[20] C. T. O'Neill, C. M. McCann, C. J. Hohimer, K. Bertoldi, and C. J. Walsh, "Unfolding textile-based pneumatic actuators for wearable applications," *Soft Robot.*, vol. 9, no. 1, pp. 163–172, Feb. 2022.

[21] J. Nassour, F. H. Hamker, and G. Cheng, "High-performance perpendicularly-enfolded-textile actuators for soft wearable robots: Design and realization," *IEEE Trans. Med. Robot. Bionics*, vol. 2, no. 3, pp. 309–319, Aug. 2020.

[22] H. K. Yap et al., "A fully fabric-based bidirectional soft robotic glove for assistance and rehabilitation of hand impaired patients," *IEEE Robot. Autom. Lett.*, vol. 2, no. 3, pp. 1383–1390, Jul. 2017.

[23] M. Feng, D. Yang, and G. Gu, "High-force fabric-based pneumatic actuators with asymmetric chambers and interference-reinforced structure for soft wearable assistive gloves," *IEEE Robot. Autom. Lett.*, vol. 6, no. 2, pp. 3105–3111, Apr. 2021.

[24] D. C. F. Li, Z. Wang, J. Zhou, and Y.-H. Liu, "Honeycomb jamming: An enabling technology of variable stiffness reconfiguration," *Soft Robot.*, vol. 8, no. 6, pp. 720–734, Dec. 2021.

[25] W. Chen et al., "Soft exoskeleton with fully actuated thumb movements for grasping assistance," *IEEE Trans. Robot.*, vol. 38, no. 4, pp. 2194–2207, Aug. 2022.

[26] G. I. Bain, N. Polites, B. G. Higgs, R. J. Heptinstall, and A. M. McGrath, "The functional range of motion of the finger joints," *J. Hand Surg.*, vol. 40, no. 4, pp. 406–411, 2015.

[27] M. J. Barakat, J. Field, and J. Taylor, "The range of movement of the thumb," *Hand*, vol. 8, no. 2, pp. 82–179, 2013.

[28] P. Tran et al., "FLEXotendon glove-III: Voice-controlled soft robotic hand exoskeleton with novel fabrication method and admittance grasping control," *IEEE/ASME Trans. Mechatronics*, vol. 27, no. 5, pp. 3920–3931, Oct. 2022.

[29] T. Bützer, O. Lambercy, J. Arata, and R. Gassert, "Fully wearable actuated soft exoskeleton for grasping assistance in everyday activities," *Soft Robot.*, vol. 8, no. 2, pp. 128–143, Apr. 2021.

[30] J. Lai, A. Song, K. Shi, Q. Ji, Y. Lu, and H. Li, "Design and evaluation of a bidirectional soft glove for hand rehabilitation-assistance tasks," *IEEE Trans. Med. Robot. Bionics*, early access, Jul. 7, 2023, doi: 10.1109/TMRB.2023.3292414.

[31] M. Uludag, O. Ulkir, I. Ertugrul, and E. Kaplanoglu, "Design, fabrication, and experiments of a soft pneumatic gripper with closed-loop position control," *J. Test. Eval.*, vol. 51, no. 5, Sep. 2023, Art. no. 20220378.